

# Morphology and Thermal/Mechanical Properties of Alkyl-Imidazolium-Treated Rectorite/Epoxy Nanocomposites

Linxi Hou, Yan Liu

Department of Polymer Materials, Faculty of Materials Science and Chemical Engineering, NingBo University, NingBo, 315211, China

Received 25 September 2010; accepted 21 August 2011

DOI 10.1002/app.35496

Published online in Wiley Online Library (wileyonlinelibrary.com).

**ABSTRACT:** A novel organic rectorite (OREC) was prepared by treating the natural sodium-rectorite (Na-REC) with ionic liquid 1-hexadecyl-3-methylimidazolium bromide ( $[C_{16}mim]Br$ ). X-ray diffraction (XRD) analysis showed that the interlayer spacing of the OREC was expanded from 2.23 nm to 3.14 nm. Furthermore, two types of OREC/epoxy nanocomposites were prepared by using epoxy resin (EP) as matrix, 2-ethyl-4-methylimidazole (2-E-4-MI) and tung oil anhydride (TOA) as curing agents, respectively. XRD and transmission electron microscope (TEM) analysis showed that the intercalated nanocomposite was obtained with addition of the curing agent 2-E-4-MI, and the exfoliated nanocomposite was obtained with addition of the

curing agent TOA when the OREC content was less than 2 wt %. For the exfoliated nanocomposite, the mechanical and thermal property tests indicated that it had the highest improvement when OREC content was 2 wt% in EP. Compared to pure EP, 60.3% improvement in tensile strength, 26.7% improvement in bending strength, 34% improvement in bending modulus, 14°C improvement in thermal decomposition temperature ( $T_d$ ) and 5.7°C improvement in glass transition temperature ( $T_g$ ) were achieved. © 2012 Wiley Periodicals, Inc. *J Appl Polym Sci* 000: 000–000, 2012

**Key words:** epoxy resin; rectorite; ionic liquid; nanocomposites; morphology; thermal/mechanical properties

## INTRODUCTION

Cured epoxy resins (EPs) have been widely used as matrix composite materials, coatings, and adhesives due to their good mechanical properties, electrical characteristics and chemical resistance.<sup>1–3</sup> However, the major problems with EPs for their further application are their brittleness, low impact strength and easy cracking.<sup>4–6</sup>

Recently, layered silicate clay/epoxy nanocomposites have attracted increasing interests from both scientific and industrial perspectives because they exhibit excellent performances compared with traditional composites, including mechanical properties, higher thermal stabilities, improved gas barrier properties,<sup>7–9</sup> and so on. Among the clays, rectorite (REC) is a kind of regular interstratified clay consisting of a muscovite-like layer and a montmorillonite-like layer in ratio of 1 : 1. It is worth further investigation in view of its many particular properties such as good dispersion, cation exchange performance, high temperature resistance, and good gas barrier property. But untreated clay

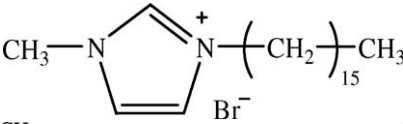
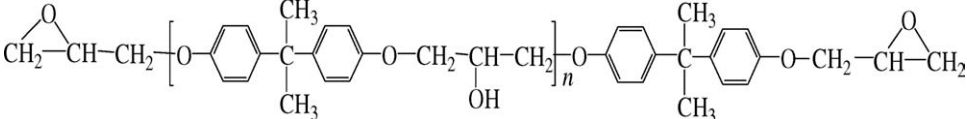
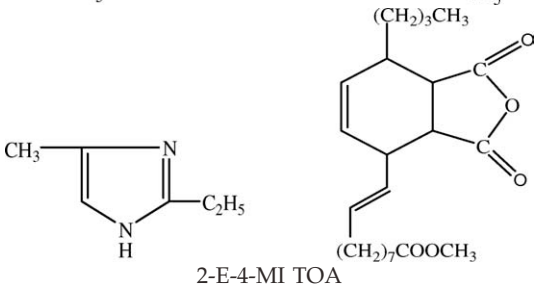
could not be dispersed well in polymeric matrix because of its natural hydrophilicity and incompatibility with organic polymers, so it must be treated with organic modifier prior to blending with organic polymers. A significant limitation of the current quaternary alkyl ammonium treatments for organic rectorite (OREC) is low thermal stability. They have been observed to have onset of Hoffmann thermal degradation at 180°C,<sup>10</sup> involving the breakage of C–N bond in the alkyl ammonium. The production of low molecular weight products and the structure change of the surfactant would change the interfacial interaction and thermodynamics of the system, consequently affecting the physical and mechanical properties of the prepared nanocomposite. Most imidazolium-based ionic liquids containing long chain cations have been proved to possess higher thermal stabilities than alkyl ammonium,<sup>11–13</sup> and were employed as clay (mostly montmorillonite) modifier in order to obtain enhanced thermal stability of the organoclay and nanocomposites. There are some reports on the alkyl-imidazolium-treated clay for the nanocomposite preparation from the thermoplastic matrixes, including nylon,<sup>14</sup> polyolefin,<sup>15–17</sup> polyester.<sup>12</sup> Few studies have been reported on the thermosetting EP nanocomposite modified with the alkyl-imidazolium-treated clay.

The goal of this investigation is to obtain the exfoliated OREC/EP nanocomposite with improved thermal stabilities and mechanical properties prepared

Correspondence to: Y. Liu (houlinxi@nbu.edu.cn).

Contract grant sponsors: Fresh Talent Initiative of Zhejiang Province, Ningbo University (K.C. Wang Magna Fund).

TABLE I  
The Structure of Organic Modifier, Epoxy Resin, and Curing Agents

Reagents	Structure
[C <sub>16</sub> mim]Br	
E-51	
Curing agent	 2-E-4-MI TOA

with the alkyl-imidazolium-treated REC. In this paper, OREC was prepared with ionic liquid 1-hexadecyl-3-methylimidazolium bromide ([C<sub>16</sub>mim]Br). And two types of OREC/EP nanocomposites were obtained with 2-ethyl-4-methylimidazole (2-E-4-MI) and tung oil anhydride (TOA) as curing agents, respectively. The effect of the OREC content and curing agent type was studied on the exfoliation behaviors of the nanocomposites, and the thermal stabilities and mechanical properties were further discussed.

## EXPERIMENTAL

### Materials

Industrial grade sodium-rectorite (Na-REC), with a cation exchange capacity (CEC) of 48 mmol/100 g, was supplied by Zhongxiang Rectorite, Wuhan, China. [C<sub>16</sub>mim]Br (chemically pure) was purchased from Lanzhou Institute of Chemical Physics. Industrial grade EP was diglycidyl ether of bisphenol A, with an average molecular weight of 390 and equivalent of 0.48–0.54 eq/100 g, obtained from Chemical plant in Wuxi Adjani. Industrial grade TOA was provided by Yangzhou Chemical and chemically pure 2-E-4-MI was import-packing. The structures of the organic modifier, resin and curing agents are illustrated in Table I.

### Experimental procedures

#### Organic modification of REC

Totally, 2 g Na-REC was dispersed in a certain amount (13.3, 20, 40, or 100 mL) of distilled water at room temperature for 1 h using a motor stirrer. The

pH value (3, 5, 7, 9, or 11) of the suspension was then adjusted with 0.1 mol/L HCl/NaOH aqueous solution at a certain temperature (40, 50, 60, 70, or 80°C). Calculated amount [C<sub>16</sub>mim]Br ([C<sub>16</sub>mim]Br/REC stoichiometric ratio of 0.5 : 1, 1 : 1, 1.5 : 1, 2 : 1, or 3 : 1) was dissolved in a mixture of ethanol and deionized water (4 : 1 v/v) and added dropwise to the slurry under stirring. The exchange reaction lasted for a certain period of time (1, 2, 4, 6, or 8 h) at the constant temperature. The OREC was then collected by vacuum filtration and washed thoroughly with distilled water until Br<sup>-</sup> was not detected with 0.1 mol/L AgNO<sub>3</sub> solution, finally dried under vacuum at 90°C for 24 h. The stoichiometric ratio (*n*) of organic modifier and REC is calculated from the following equation: [CEC (mmol)/100 (g) × weight of REC (g) × *n*] = [weight of modifier (g) × 1000/molecular weight of modifier (g/mol)].

#### Preparation of OREC / EP nanocomposites

A desired amount of OREC was dispersed in EP at 70°C using a motor stirrer. After being mixed for 4h, the mixtures were cooled to 60°C. (1) 3.5 g 2-E-4-MI per 100 g resin was added into the resin under thorough mixing. The mixture were then degassed at 60°C for 30 min and poured into a preheated mould in an oven and cured at 80°C for 2 h and postcured at 120°C for 4 h. (2) Curing agent TOA and accelerator 2-E-4-MI were added under stirring, with the mixture ratio as follow: 150 parts anhydride and 1 parts imidazole per 100 parts resin. Then the well-mixed sample was degassed at 60°C for 30 min and poured into a preheated mould in an oven and cured at 120°C for 2 h and postcured at 150°C for 3 h.

**TABLE II**  
**The Effect of the Raw Material Ratio, Slurry, pH Value, Reaction Temperature, and Reaction Time on Clay CEC**

	[C <sub>16</sub> mim]Br/REC stoichiometric ratio (5%, pH = 7, 50°C, 4 h)					The slurry concentration (%) (1 : 1, pH = 7, 50°C, 4 h)		
	0.5 : 1	1 : 1	1.5 : 1	2 : 1	3 : 1	2	10	15
C (wt %)	6.35	10.7	12.56	13.02	14.68	10.43	10.95	11.03
The equivalent CEC (mmol/100g)	26.46	44.58	52.33	54.25	61.17	43.44	45.63	45.96
	pH value (1 : 1, 5%, 50°C, 4 h)				The reaction temperature (°C) (1 : 1, 5%, pH = 7, 4 h)			
	3	5	9	11	40	60	70	80
C (wt %)	10.47	10.64	10.91	10.99	10.63	10.78	10.95	10.75
The equivalent CEC (mmol/100g)	43.63	44.33	45.46	45.81	44.29	44.92	45.63	44.79
	The reaction time (h) (1 : 1, 5%, pH = 7, 50°C)							
	1		2		6		8	
C (wt %)	8.82		10.06		10.72		10.74	
The equivalent CEC (mmol/100 g)	36.74		41.92		44.67		44.75	

### Measurements and characterization

The CEC of REC in operation conditions was determined by detecting the C content in OREC with a Perkin-Elmer 2400II elemental analyzer in a pure oxygen environment. FTIR spectra of REC, OREC, and nanocomposites were obtained using a Shimadzu FTIR-8900 infrared spectrometer with a scanning range of 400–4000 cm<sup>-1</sup>. X-ray diffraction (XRD) measurements on clay powder samples and nanocomposites were performed using a UltimaIII X-ray diffractometer with Cu-K<sub>α</sub> radiation ( $\lambda = 1.5418 \text{ \AA}$ ) from 0 to 30° at a scanning rate of 0.5° (2 $\theta$ )/min. The microstructures of nanocomposites were imaged using an H-7650 transmission electron microscope (TEM) under an accelerated voltage of 150 kV. The morphologies of the tensile fracture surfaces were observed using an S-3400 N scanning electron microscopy (SEM) under an accelerated voltage of 10 kV. Thermogravimetric analysis (TGA) of the nanocomposites were carried out on a Seiko EXSTAR 6300 thermal analyzer at a heating rate of 10°C/min in a nitrogen atmosphere, scanning range 50–600°C. The glass transition temperature ( $T_g$ ) of the nanocomposites were studied on a Perkin Elmer DMA 7e at a heating rate of 5°C/min, scanning range 30 to 200°C. The mechanical properties of nanocomposites, including tensile strength, bending strength, were measured using a SUNS CMT4104 electronic universal testing machines, the samples with the dimensions of 80 mm × 40 mm × 3.5 mm.

## RESULTS AND DISCUSSION

### Organic modification of REC

#### Element analysis

To determine the effect of the raw material ratio, slurry concentration, reaction temperature, reaction

time, pH value on the CEC, the reaction was performed with [C<sub>16</sub>mim]Br/REC stoichiometric ratio of 0.5 : 1, 1 : 1, 1.5 : 1, 2 : 1, or 3 : 1, slurry concentration of 2, 5, 10, or 15%, pH value of 3, 5, 7, 9, or 11, reaction temperature at 40, 50, 60, 70, or 80°C, reaction time for 1, 2, 4, 6, or 8 h.

The clay CEC under each condition was analyzed by element analysis. The results (Table II) show that the measured value of CEC increases with [C<sub>16</sub>mim]Br/REC stoichiometric ratio and slurry concentration increasing. It is due to the cation exchange reaction in the aqueous solution:  $\text{Rec-Na}_n + n [\text{C}_{16}\text{mim}]\text{Br} = \text{Rec}[\text{C}_{16}\text{mim}]_n + n\text{NaBr}$ , where  $\text{Rec-Na}_n$  is Na-REC,  $\text{Rec}[\text{C}_{16}\text{mim}]_n$  is OREC. The increasing of the [C<sub>16</sub>mim]Br content will promote the forward reaction, thus the CEC increases. As the stoichiometric ratio of [C<sub>16</sub>mim]Br/REC increases above 1 : 1, the CEC is up to 52.33 mmol/100 g (>48 mmol/100 g), the “over CEC” is due to the excess van der Waals adsorption between alkyl chains on the clay surface. Meanwhile, there are more exchangeable cations per unit volume in the higher concentration slurry, which has a positive effect on the cation exchange reaction. And a little higher clay CEC was observed as the pH value increases. It results from the increase in the OH<sup>-</sup> numbers and negative charges absorbed by the clay surface in slurry solution at a higher pH value.<sup>18</sup> However, the reaction temperature within the experimental range has little influence on the measured CEC, indicating that the cation exchange reaction can take place completely at low temperature. Besides, the clay CEC would reach to a steady state when the reaction time prolonged over 4 h, suggesting that the cation exchange reaction could complete at a fast rate within 4 h.

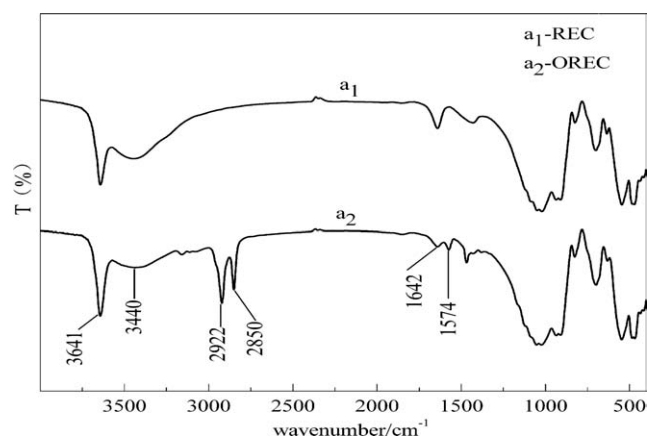


Figure 1 FTIR spectra of REC and OREC.

In addition, in the organic modification process of REC, too much froth of  $[C_{16}mim]Br$  would form in the reaction system when the stoichiometric ratio of  $[C_{16}mim]Br/REC$  increased over 1.5 : 1, which may cause difficulties in the post-treatment. And water-swelling REC could not disperse well when the slurry concentration was over 10%. On the basis of the above phenomena and analysis, the optimum process condition for the organic modification of REC is determined as follow: the stoichiometric ratio of  $[C_{16}mim]Br/REC$  is 1.5 : 1, the slurry concentration 5%, reaction temperature  $50^{\circ}C$ , reaction time 4 h, pH value 9.

#### FTIR spectra analysis

Figure 1 shows the FTIR spectra of Na-REC and OREC. In the spectrum of Na-REC shown in 1a<sub>1</sub>, sharp peak around  $3641\text{ cm}^{-1}$  is assigned to stretching vibration of hydroxyl in free hydrogen bond, the broad band at  $3440\text{ cm}^{-1}$  is assigned to the free inter-layer water. Si—O stretching vibration is observed at  $1024\text{ cm}^{-1}$ , and the band between  $540\text{ cm}^{-1}$  and  $470\text{ cm}^{-1}$  is assigned to Al—O and Mg—O stretching

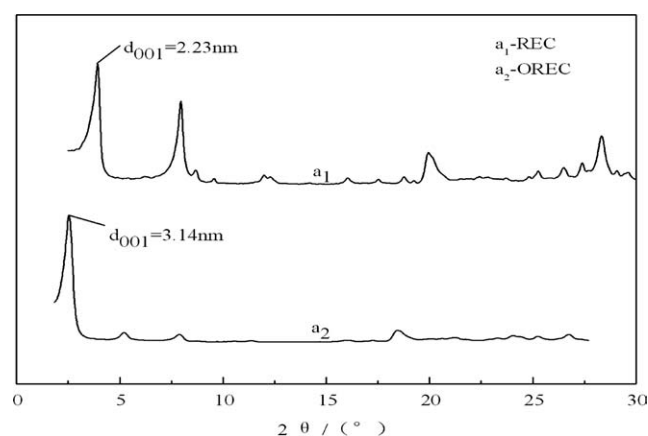


Figure 2 XRD patterns of REC and OREC.

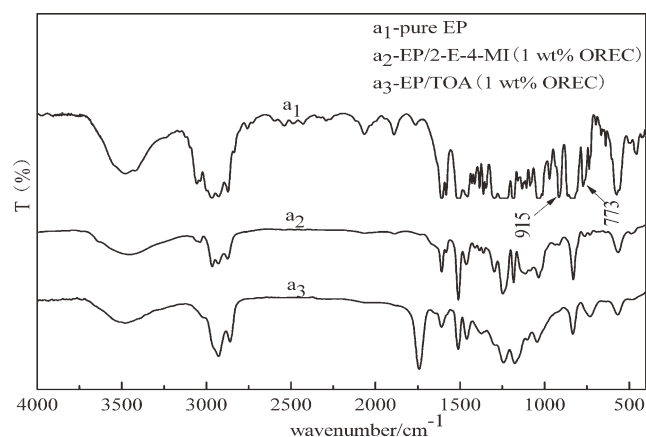


Figure 3 FTIR spectra of different samples.

vibrations. In the spectrum of OREC shown in 1a<sub>2</sub>, the strong peaks around  $2922\text{ cm}^{-1}$  and  $2850\text{ cm}^{-1}$  are due to methyl and methylene groups stretching, the peaks at  $1642\text{ cm}^{-1}$  and  $1574\text{ cm}^{-1}$  are due to C=C and C=N bonds stretching, respectively. This indicates that the ionic liquid has successfully entered into the clay interlayer, and REC has been converted from hydrophilic to hydrophobic.

#### XRD analysis

Figure 2 shows the XRD patterns of Na-REC and OREC. In the pattern of Na-REC shown in 2a<sub>1</sub>, the sharp  $d_{001}$  peak indicates that the Na-REC has a well-crystallized structure, with a  $d$ -spacing of 2.23 nm. In the pattern of OREC shown in 2a<sub>2</sub>, it can be seen that the  $d$ -spacing of OREC is widened to 3.14 nm. Therefore, it can be concluded that the natural Na-REC has been successfully modified with ionic liquid  $[C_{16}mim]Br$ , and its interlayer spacing is expanded.

#### Structural analysis of nanocomposites

##### FTIR spectra analysis

Figure 3 shows the FTIR spectra of uncured pure EP and the two kinds of nanocomposites containing 1wt % OREC cross-linked with 2-E-4-MI and TOA, respectively. The epoxy group absorption peaks are observed at  $915\text{ cm}^{-1}$  and  $773\text{ cm}^{-1}$  in pure epoxy resin [Fig. 3(a<sub>1</sub>)]. They become very weak in the nanocomposite cured with 2-E-4-MI [Fig. 3(a<sub>2</sub>)], and disappear completely in the nanocomposite cured with TOA [Fig. 3(a<sub>3</sub>)], indicating that the curing reactions have taken place in the two curing systems. In addition, it can be found that the —OH peak in OREC at  $3641\text{ cm}^{-1}$  (refer to Fig. 1) disappears in the two kinds of nanocomposites, which shows that hydrogen bond networks form by hydroxyl interaction between OREC and EP matrix.<sup>19</sup>

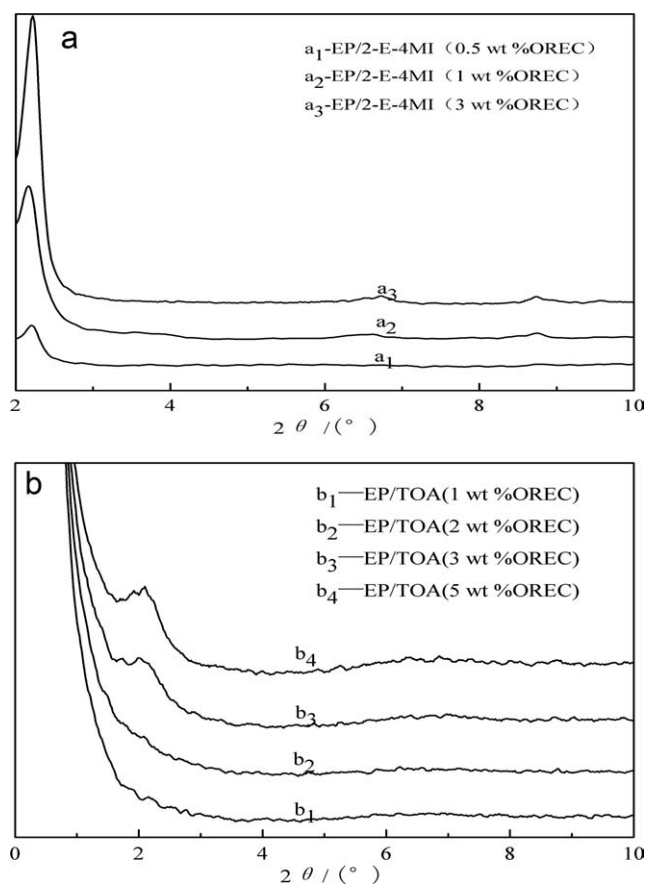
### XRD analysis

Figure 4 shows the XRD patterns of the nanocomposites containing different OREC content. In the pattern of nanocomposite cross-linked with 2-E-4-MI shown in 4a, it can be observed that all the  $d_{001}$  diffraction peaks appear at  $2\theta = 2.2^\circ$  corresponding to a  $d$ -spacing of 4 nm, and the intensity of the peaks increase as OREC loading increases. This indicates that the EP molecules have entered into the clay gallery and participated in the curing reaction, forming an intercalated nanocomposite. In the pattern of nanocomposite cross-linked with TOA shown in 4b, no diffraction peak is detected when the OREC content is lower than 2 wt %, indicating that the clay layers are exfoliated without regular repeat distance. According to the minimum testing value  $2\theta = 0.8^\circ$ , it can be calculated that the interlayer spacing is greater than 11 nm. It is considered that a large amount of epoxy monomers enter into the clay gallery and participate in the cross linking reaction with TOA in the intragallery. A lot of reaction heat release and overcome the van der Waals interaction energy of the clay layers, which lead to the galleries expanding. When the galleries exfoliate completely, an exfoliated nanocomposite is formed finally. However, the diffraction peaks appear again when the OREC content is higher than 3 wt %. It indicates that the clay galleries in the nanocomposite are difficult to exfoliate at higher OREC loading, and only the intercalated nanocomposite can be formed.

To form an exfoliated nanocomposite, there must be plenty of epoxy monomers to take part in the curing reaction in the intragallery, and the intragallery polymerization rate should be comparable with or larger than the extragallery polymerization rate,<sup>20</sup> giving out enough curing heat to overcome the van der Waals attractive energy between the clay layers. Consequently, the clay layers would be fully exfoliated and dispersed well in the EP matrix. Liquid TOA with high polarity has a good compatibility with OREC. As a high-temperature curing agent, its long flexible long-chain branches will be able to penetrate into the clay galleries easily at a high temperature before the curing system reaches the gel point, which will accelerate the intragallery polymerization, giving out enough heat and expanding the clay interlayer space. Meanwhile, the epoxy molecules outside will further move into the intragalleries while the curing reaction is taking place, resulting in a further expanded layer space.

### TEM analysis

Figure 5 displays the TEM micrographs of the two kinds of nanocomposites with 1 wt % OREC. In the photo of nanocomposite cross-linked with 2-E-4-MI



**Figure 4** XRD patterns of different samples. (a) 2-E-4-MI as curing agent; (b) TOA as curing agent.

shown in 5a, the black lines are made up of the clay layers and the white area is the EP matrix. It can be seen that the clay layers arrange regularly, with the interlayer spacing enlarged to be about 4 nm, forming the intercalated nanocomposite. In the photo of nanocomposite cross-linked with TOA shown in 5b, the clay layers are disorderly separated to be 12–20 nm and dispersed well in the EP matrix, forming the exfoliated and quasi-exfoliated nanocomposite. The clay morphologies are compatible with the XRD results.

### Property analysis of nanocomposites

#### Mechanical property analysis

Figure 6 shows the tensile strength (6a), bending strength (6b), and bending modulus (6c) of the exfoliated nanocomposites cured with TOA with different OREC content. It can be seen that the nanocomposite exhibits best mechanical performances when the OREC content reaches 2 wt %. As the OREC content increases to 2 wt %, the tensile strength was improved from 18.9 to 30.3 MPa, by 60.3%; the bending strength from 53.34 to 67.59 MPa, by 26.7%; the bending modulus from 2.12 to 2.84 GPa, by 34%, as compared with the neat EP. But each indicator begins

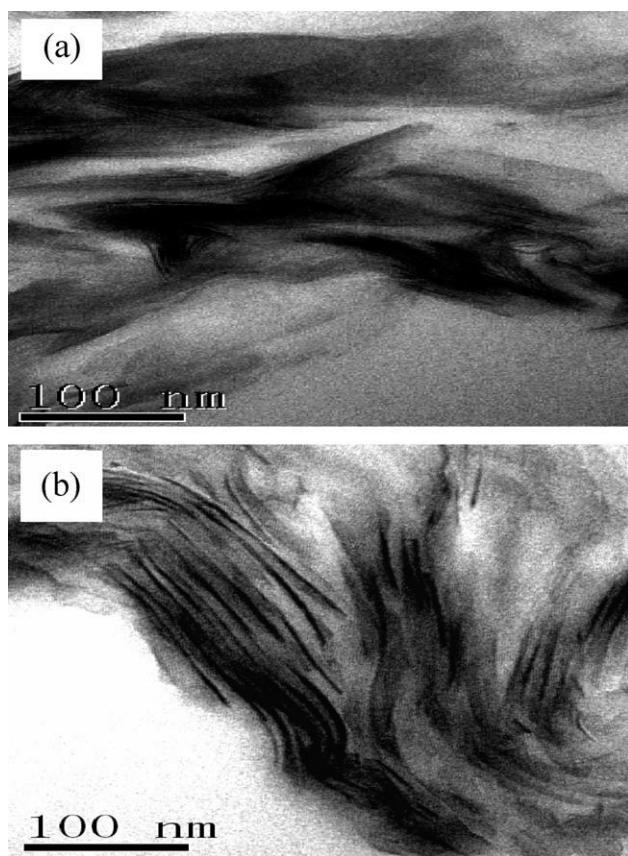


**Figure 5** TEM micrographs of two kinds of nanocomposites with 1 wt % OREC. (a) Nanocomposite cured with 2-E-4-MI; (b) Nanocomposite cured with TOA.

to drop with further increasing OREC content. The effect mentioned above can be explained as follow. When the OREC loading is relatively low (below 2 wt %), the well-dispersed clay layers can reach a single-layer exfoliation and quasi exfoliation, and the exfoliated nanolayers interface could be combined with the matrix by a strong chemical bonding. Besides, with high strength and stiffness, the nanolayers play a role of the stress concentration sites in the epoxy matrix, which may lead to a lot of crazing and absorb some energy. On the other hand, the nanolayers can interact with the growing crack front, and resist the microcrack from propagating into macrocrack.<sup>21–23</sup> As a result, the mechanical properties of nanocomposite are improved. However, at higher OREC contents (above 3 wt %), the intercalated structures disperse inhomogeneously in the epoxy matrix and form agglomerate particles, which may induce the formation of macrocracks. Therefore the decrease in the mechanical properties of nanocomposites was observed.

To elucidate the reasons for the fracture behaviors, the tensile fracture surfaces were examined by using SEM. Figure 7 displays the SEM micrographs of the fracture surfaces for the neat EP, the nanocomposites containing 1 and 5 wt % OREC. Figure 7(a) shows

that the fracture surface of the neat EP is relatively smooth with cracks in different planes but almost parallel to the crack-propagation direction. It is a typical fractograph feature of brittle fracture behavior, accounting for the low fracture toughness of the unfilled epoxy. On the contrary, the fracture surface of the nanocomposite with 1 wt % OREC [Fig. 7(b)] appears to be much rougher with the distorted cracks in different propagation direction. This indicates a typical fractograph feature of tough fracture behavior, which accounts for the improvement on fracture

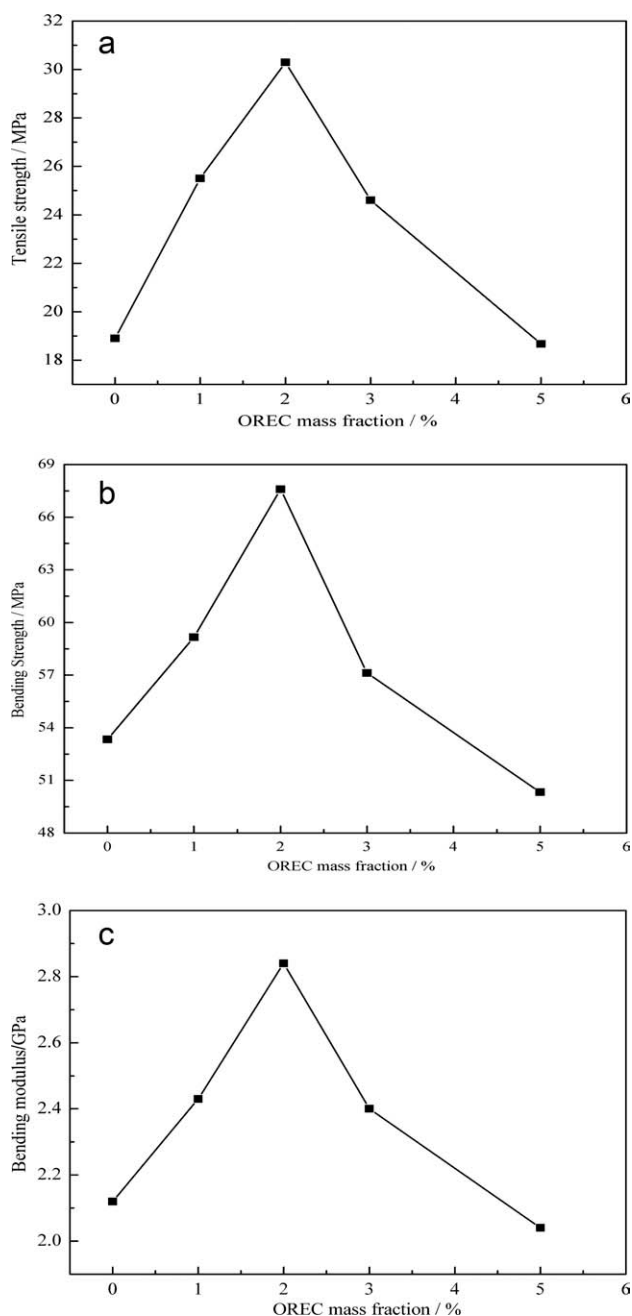


**Figure 6** The effect of OREC content on the mechanical properties of the nanocomposites cured with TOA (a) Tensile strength; (b) Bending strength; (c) Bending modulus.

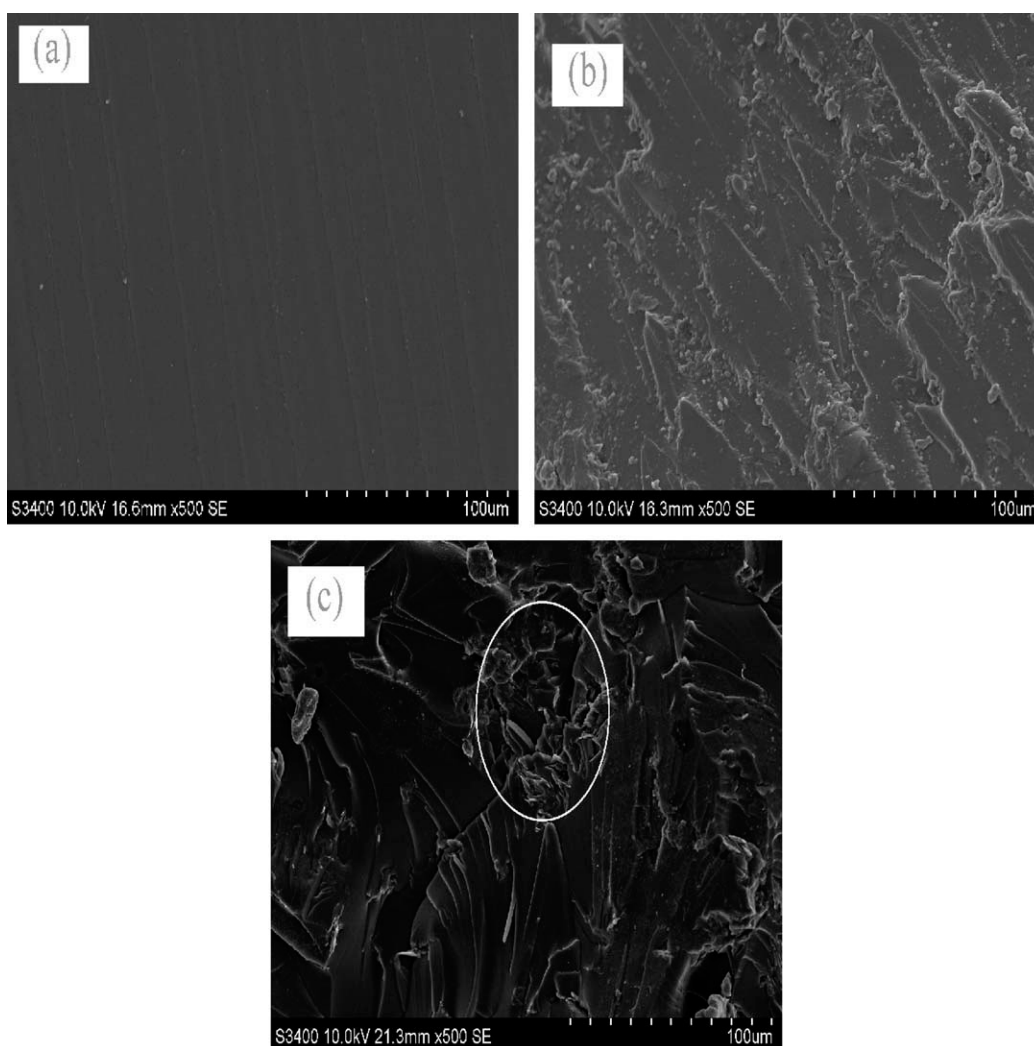


**Figure 7** SEM micrographs of pure EP and EP/TOA nanocomposite with 1 wt % and 5 wt % OREC (a) Pure EP; (b) EP/TOA with 1 wt % OREC; (c) EP/TOA with 5 wt % OREC.

toughness for the nanocomposite. Obviously, the formation of the surface roughness is attributed to the exfoliated clay layers in the epoxy matrix, the stress concentration sites, which may interact with the growing crack front, and alter their path from the straight unperturbed propagation direction.<sup>24</sup> Thus, the cracks are deflected into the rougher regions surrounding them. Furthermore, clay agglomerates can be observed on the fracture surface (shown at the circle) of nanocomposite with 5 wt % OREC [Fig. 7(c)]. It indicates that the clay particles are prone to form agglomerate particles with size of about 55  $\mu\text{m}$  at higher OREC loading, and the uneven disperse in the epoxy matrix leads to the formation of macrocracks. On the basis of the above analysis, the mechanical properties of nanocomposites would decrease with higher clay content.

#### Thermal property analysis

Figure 8 shows the TG and DMA curves of the exfoliated nanocomposites with different OREC content

cured with TOA. The thermal decomposed temperature ( $T_d$ , the temperature of degradation at which the weight loss is 5 wt %) is shown in 8a, and the glass transition temperature ( $T_g$ ) is shown in 8b. It can be clearly seen that  $T_d$  and  $T_g$  of the nanocomposites reach a maximum value as the OREC content increase to 2 wt %. Compared with the pure EP,  $T_d$  increases from 350°C to 364°C, by 14°C;  $T_g$  increases from 111.8°C to 117.5°C, by 5.7°C. The results may be owing to the following reasons. The thermal performances of the nanocomposite depend on the dispersion state of the OREC in the epoxy matrix. At relatively low OREC loading (below 2 wt %), all the clay monolayers disperse uniformly in the epoxy matrix, and the confinement of the intercalated polymer chains within the clay galleries prevents the segmental motions of the polymer chains,<sup>25</sup> causing the reduction in the free volume of the matrix. Consequently, the thermal performances of the nanocomposites are enhanced. However, with further addition of OREC (above 3 wt %), the nonuniform

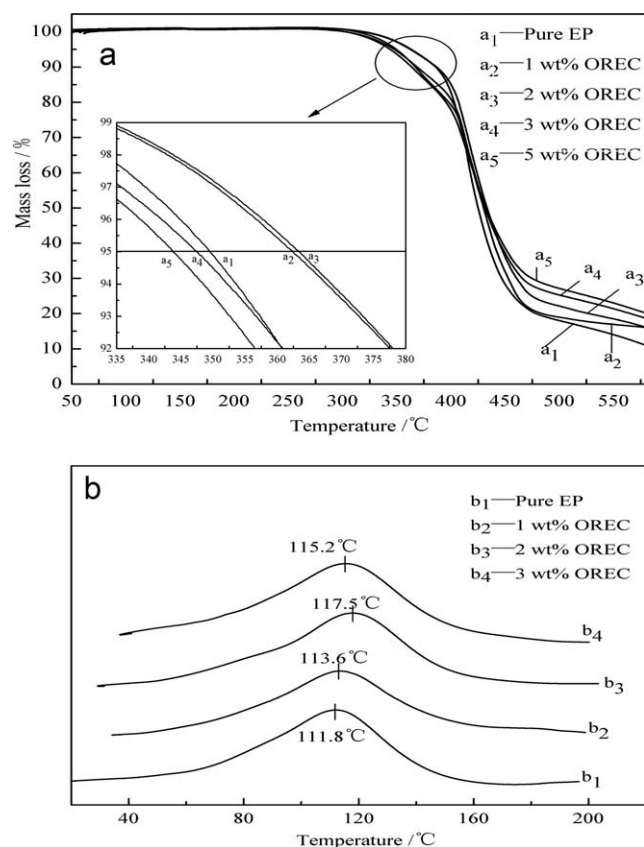


**Figure 8** TG and DMA curves of nanocomposites with different OREC mass fraction. (a) TG curves; (b) DMA curves.

dispersion and agglomerates may reduce the cross-link density of the matrix, which cause the degradation of thermal performances of the nanocomposite.

## CONCLUSIONS

A novel OREC was prepared by sodium–rectorite and ionic liquid 1-hexadecyl-3-methylimidazolium bromide, and its interlayer spacing was expanded from 2.23 to 3.14 nm. Two types of OREC/EP nanocomposites were obtained from the prepared OREC and epoxy resin cross-linked with 2-ethyl-4-methylimidazole and tung oil anhydride as curing agents, respectively, and their structure characteristics and properties were investigated. It proves that different curing agents result in different structural nanocomposites. With addition of the curing agent 2-ethyl-4-methylimidazole, the intercalated nanocomposite was obtained; with addition of the curing agent tung oil anhydride, the exfoliated nanocomposite was obtained when the OREC content was less than 2 wt %. Compared with pure epoxy resin, the exfoliated OREC/epoxy nanocomposite containing 2 wt %

OREC has superior mechanical and thermal properties. The novel alkyl-imidazolium-treated rectorite could be also applicable to the preparation of other types of polymer-based nanocomposites with high processing temperatures.

The author gratefully acknowledges the support of K.C. Wong Education Foundation and K.C. Wong Magna Fund, Hong Kong.

## References

- Wang, L.; Wang, K.; Chen, L.; He, C. B.; Zhang, Y. W. *Polym Eng Sci* 2006, 46, 215.
- Zilg, C.; Thomann, R.; Finter, J.; Mulhaupt, R. *Macromol Mater Eng* 2000, 280/281, 41.
- Lv, J. K.; Ke, Y. C.; Qi, Z. N. *Acta Mater Comp Sin* 2002, 19, 117.
- Bakar, M.; Kostrzema, M.; Okulska-Bożek, M.; Jaxewicz, E. *J Appl Polym Sci* 2010, 119, 752.
- Suguna Lakshmi, M.; Narmadha, B.; Reddy, B. S. R. *Polym Degrad Stabil* 2008, 93, 201.
- Yang, J. P.; Yang, G.; Xu, G. S. *Compos Sci Technol* 2007, 67, 2934.
- Chen, K. H.; Yang, S. M. *J Appl Polym Sci* 2002, 86, 414.
- Osman, M. A.; Mittal, V.; Morbidelli, M.; Suter, U. S. *Macromolecules* 2004, 37, 7250.
- Zhang, K. L.; Wang, L. X.; Wang, F.; Wang, G. J.; Li, Z. B. *J Appl Polym Sci* 2004, 91, 2649.
- Xie, W.; Gao, Z.; Pan, W. P.; Hunter, D.; Singh, A.; Vaia, R. *Chem Mater* 2001, 13, 2979.
- Awad, W. H.; Gilman, J. W.; Nyden, M.; Harris, R. H.; Sutto, T. E.; Callahan, J.; Trulove, P. C.; DeLong, H. C.; Fox, D. M. *Thermochimi Acta* 2004, 409, 3.
- Trulove, P. C.; Fox, D. M.; Award, W. H.; Gilman, J. W.; Davis, C. D.; Sutto, T. E.; Maupon, P. H.; DeLong, H. C. *Ionic Liquids IV*; American Chemical Society: Washington D. C., 2007.
- Kim, N. H.; Malhotra, S. V.; Xanthos, M. *Micropor Mesopor Mater* 2006, 96, 29.
- Gilman, J. W.; Awad, W. H.; Davis, R. D.; Shields, J.; Harris, R. H.; Davis, C.; Morgan, A. B.; Sutto, T. E.; Callahan, J.; Trulove, P. C.; DeLong, H. C. *Chem Mater* 2002, 14, 3776.
- Ding, Y. S.; Guo, C. Y.; Dong, J. Y.; Wang, Z. G. *J Appl Polym Sci* 2006, 102, 4314.
- Ha, J. U.; Xanthos, M. *Polym Compos* 2009, 30, 534.
- Mittal, V. *Eur Polym J* 2007, 43, 3727.
- Ke, Y. C.; Stroeve, P. *Polymer-Inorganic Nanocomposites*; Chemical Industry Press: Beijing, 2003.
- Liu, L. M.; Zhang, M.; Fang, P. F.; Wang, B.; Zhang, S. P. *Acta Polym Sin* 2005, 1, 128.
- Messersmith, P. B.; Giannelis, E. P. *Chem Mater* 1994, 6, 1719.
- Wang, K.; Chen, L.; Wu, J. S.; Toh, M. L.; He, C. B.; Yee, A. F. *Macromolecules* 2005, 38, 788.
- Liu, W. P.; Hoa, S. V.; Pugh, M. *Compos Sci Technol* 2005, 65, 307.
- Yuan, L.; Ma, X. Y.; Gu, A. J.; Yan, H. X.; Liang, G. Z.; Wang, W.; Wu, J. Y. *Polym Advan Technol* 2009, 20, 826.
- Liu, T. X.; Tjiu, W. C.; Tong, Y. J.; He, C. B.; Goh, S. S.; Chung, T. S. *J Appl Polym Sci* 2004, 94, 1236.
- Yeh, J. M.; Huang, H. Y.; Chen, C. L.; Su, W. F.; Yu, Y. H. *Surf Coat Tech* 2006, 200, 2753.